Comparison of extended Jones matrices for twisted nematic liquid-crystal displays at oblique angles of incidence

F. H. Yu* and H. S. Kwok

Center for Display Research and Department of Electronic and Electrical Engineering, Hong Kong University of Science & Technology, Clear Water Bay, Kowloon, Hong Kong

Received April 12, 1999; accepted May 26, 1999; revised manuscript received June 16, 1999

Detailed formulas were derived by using Yeh's formulation of the extended 2 × 2 Jones matrix and applied to twisted nematic liquid-crystal displays at oblique angles of incidence. Numerical comparisons of this extended Jones matrix method with the exact 4 × 4 Berreman matrix and with the extended Jones matrix of Lien are presented. The various extended Jones matrix formulations differ in their approach to boundary-condition matching between the model birefringent layers. We show that Yeh's version is a more accurate approximation to the full 4 × 4 matrix. This extended Jones matrix method is fast, direct, and simple. It is also physically more intuitive. © 1999 Optical Society of America [S0740-3232(99)00711-5]

OCIS codes: 160.3710, 230.3720, 120.2040, 000.4430, 080.2730.

1. INTRODUCTION

Numerical simulation is an important tool in the design and the optimization of the electro-optical properties of liquid-crystal displays (LCD's). The optical properties of commonly used twisted nematic (TN)[1,2] and supertwisted nematic (STN)[3] displays depend strongly on a large set of material and cell parameters. There are only a few cases where the optical properties of the LCD can be obtained analytically, a notable exception being the Mauguin modes of 90° TN displays.[4] At oblique incidence or when a voltage is applied to the cell, the problem of obtaining the transmission or reflection coefficients of any LCD has to be solved numerically.

For numerical simulations of such situations, the typical approach is to treat the LCD as a stack of N birefringent plates, with the optical axis of each plate twisted slightly from the next. N is usually a number less than 100 such that the twist angle between adjacent plates is small. Exact solutions can be obtained by Berreman's 4 × 4 matrix approach,[5] which takes into account the effects of refraction and multiple reflections of the electromagnetic wave between plate interfaces. This exact Berreman matrix calculation requires lengthy calculations, however. Over the years many approximations to this scheme have been proposed. For example, the exact Berreman matrix can be approximated by the fast 4 × 4 matrix.[6] Fabry–Perot effects associated with the 4 × 4 matrix can also be eliminated by spectral averaging.[7] These methods have been found to be more practical in reducing the computation time while maintaining a reasonable accuracy.

In another approach there were several attempts to generalize or extend the 2 × 2 Jones matrix to the case of oblique angles of incidence.[8–13] Yeh first discussed the case of a single birefringent plate, using the principle of refraction of light.[8,9] The matching of boundary conditions between the isotropic and the birefringent media can be taken care of exactly. Gu and Yeh then later extended this to the case of multiple layers, including the case of LCD modeling.[10] In the case of LCD's, one has to deal with waves propagating from one birefringent material to the next. The matching of boundary conditions cannot be done exactly as in the case of the 4 × 4 matrix. Gu and Yeh's approach involved assuming fictitious zero-thickness isotropic media between the birefringent plates. With use of the principle of reflection and refraction of waves between isotropic and anisotropic layers, the modeling of LCD's can be accomplished.

On the other hand, Lien proposed another form of the extended Jones matrix, where the effects of Fresnel refraction at the plate interfaces were accounted for by matching only the electric field boundary conditions.[11] A good agreement with the exact 4 × 4 matrix was obtained. This method has been applied quite extensively in LCD modeling. However, this Lien extended Jones matrix neglected the reflected waves and assumed that only two transmitted waves were propagating in the liquid-crystal cell. Moreover, only the boundary conditions for the electric fields were considered. In a more recent, improved version, Lien introduced the "new 2 × 2 matrix," where both the magnetic field and electric field boundary conditions were taken into consideration. This was accomplished by obtaining the liquid-crystal Jones matrices with the use of electric field boundary conditions and magnetic field boundary conditions separately and then combining them in some manner.[12] The results showed an improvement over those from use of the original extended Jones matrix. In yet another approach, Lu and Saleh discussed a perturbation expansion of the 4 × 4 matrix to obtain the extended Jones matrix as a first approximation.[13] However, no detailed calculations were performed.

In this paper we shall concentrate on a comparison of the accuracies of the Lien extended Jones matrix and the Yeh extended Jones matrix in approximating the exact 4×4 Berreman matrix. Even though computing powers have improved to a point where computation time is generally not an issue for LCD modeling, we feel that it is still useful to discuss the physics of the extended Jones matrix and its appropriateness to LCD modeling. In particular, it should be interesting to compare the different approaches to boundary-condition matching. While Gu and Yeh assumed a fictitious isotropic layer between the birefringent plates,[10] Lien and Chen matched the boundary conditions from one birefringent plate to another directly.[12]

It is believed that the Gu and Yeh approach is more intuitive. Boundary-condition matching is accomplished based on wave propagation and optical reflection and refraction in any anisotropic medium. However, in the original paper of Gu and Yeh, no detailed analytical expressions for the case of LCD modeling were given.[10] Additionally, approximations were made in some of the formulas that rendered them not too accurate and unsuitable for practical LCD modeling. In this paper we shall use the Yeh 2×2 Jones matrix approach[8,9] to obtain detailed general analytical expressions for modeling the optical properties of liquid-crystal cells at arbitrary incidence angles. As in the study of Gu and Yeh, we shall use the same assumption of fictitious zero-thickness isotropic layers to accomplish boundary-condition matching.[10] Detailed numerical results will be given for the case of 90° TN cells. We shall show that the Yeh extended Jones matrix is more accurate than both the earlier and the recent version of the Lien extended Jones matrix. Thus a fast and accurate approximation of the 4×4 matrix can be used to model LCD optics.

In Section 2 we derive the generalized 2×2 Jones matrix formulation of the uniaxial medium sandwiched between two isotropic media. In Section 3 we apply this generalized 2×2 Jones matrix to the case of liquid-crystal cells at oblique angles of incidence. The analytical expressions of the transformation matrix for calculating the cell optical transmission are then derived. In Section 4 some special cases of the generalized Jones matrix are discussed. Boundary transformation matrices are then given in Section 5. Numerical comparisons of the exact 4×4 matrix, the Yeh Jones matrix, and the Lien Jones matrix are presented in Section 6. Finally, Section 7 presents the conclusions.

2. GENERALIZED 2×2 JONES MATRIX OF A UNIAXIAL MEDIUM BETWEEN TWO ISOTROPIC MEDIA

As usual, the liquid-crystal cell is treated as a stack of N birefringent plates, with each plate twisted slightly from the next. It is assumed that N is sufficiently large so that the optical axis can be regarded as constant within the plates. The main difference between the various approaches to LCD modeling lies in the way reflection and refraction are treated between the birefringent plates and in the matching of boundary conditions across the layers. The main idea of the present approach is to assume a fictitious zero-thickness isotropic medium between the birefringent plates. If these layers are of zero thickness, they should not affect the physical properties of the LCD. To derive the formulas below, one can simply imagine these isotropic layers to be finite and let the thickness collapse to zero.

With such an approach, the wave propagation problem is reduced to finding the reflection and refraction behavior of light between an isotropic and a uniaxial medium. This is different from other approaches, where one has to match the boundary conditions between two anisotropic media. While this cannot be achieved directly, Lien accomplished it by averaging two Jones matrices, which are derived by matching electric field and magnetic field boundary conditions separately.[8] The application of a zero-thickness layer enables exact boundary-condition matching. The problem is simplified further if we assume that the isotropic medium has a refractive index n_o that is the same as the ordinary index of the liquid crystal.

In the two isotropic media, one just needs to consider the **s** and **p** vectors of the incident wave. In the uniaxial medium, however, the light is represented by **o** and **e** waves. The refraction of light at the interface of the isotropic and uniaxial media can be written in matrix form as[11–13]

$$\begin{pmatrix} \mathbf{E}_e \\ \mathbf{E}_o \end{pmatrix} = \begin{bmatrix} R(\mathbf{p}, \mathbf{e}) & R(\mathbf{s}, \mathbf{e}) \\ R(\mathbf{p}, \mathbf{o}) & R(\mathbf{s}, \mathbf{o}) \end{bmatrix} \begin{pmatrix} \mathbf{E}_p \\ \mathbf{E}_s \end{pmatrix}. \tag{1}$$

In Eq. (1) $\mathbf{E}_p$ and $\mathbf{E}_s$ are the electric field components of the **p** and **s** vectors in the isotropic medium, and $\mathbf{E}_e$ and $\mathbf{E}_o$ are the electric field components of the **e** and **o** vectors in the uniaxial medium. $R(\mathbf{p}, \mathbf{e})$, $R(\mathbf{s}, \mathbf{e})$, $R(\mathbf{p}, \mathbf{o})$, and $R(\mathbf{s}, \mathbf{o})$ are the transformation coefficients of the respective vectors.

The transformation matrix for a wave propagating from an isotropic medium into a uniaxial medium and exiting to another isotropic medium is therefore given by

$$\begin{aligned} \begin{pmatrix} \mathbf{E}'_p \\ \mathbf{E}'_x \end{pmatrix} &= \begin{bmatrix} R(\mathbf{e}, \mathbf{p}) & R(\mathbf{o}, \mathbf{p}) \\ R(\mathbf{e}, \mathbf{s}) & R(\mathbf{o}, \mathbf{s}) \end{bmatrix} \\ &\quad \times \begin{bmatrix} \exp(-ik\sigma_{ez}h) & 0 \\ 0 & \exp(-ik\sigma_{oz}h) \end{bmatrix} \\ &\quad \times \begin{bmatrix} R(\mathbf{p}, \mathbf{e}) & R(\mathbf{s}, \mathbf{e}) \\ R(\mathbf{p}, \mathbf{o}) & R(\mathbf{s}, \mathbf{o}) \end{bmatrix} \begin{pmatrix} \mathbf{E}_p \\ \mathbf{E}_s \end{pmatrix} \\ &= J \begin{pmatrix} \mathbf{E}_p \\ \mathbf{E}_s \end{pmatrix}, \end{aligned} \tag{2}$$

where J is the Jones matrix for this sandwich and is given by

$$J = R_2 G R_1. \tag{3}$$

In Eq. (2) $R(\mathbf{e}, \mathbf{p})$, $R(\mathbf{o}, \mathbf{p})$, $R(\mathbf{e}, \mathbf{s})$, and $R(\mathbf{o}, \mathbf{s})$ are the coefficients of the transformation matrix from the uniaxial medium to the isotropic medium. σ_{ez} and σ_{oz} are the two eigenvalues of the **e** and **o** waves in the anisotropic medium, and h is the thickness of that layer. $\mathbf{E}'_p$ and $\mathbf{E}'_s$ are the electric field components of the **p** and **s**

vectors in the exit isotropic medium. The coefficients of matrices R_1 and R_2 are given by[11–13]

$$R(\mathbf{p}, \mathbf{e}) = R(\mathbf{e}, \mathbf{p}) = \mathbf{p} \cdot \mathbf{e},$$
$$R(\mathbf{s}, \mathbf{e}) = R(\mathbf{e}, \mathbf{s}) = \mathbf{s} \cdot \mathbf{e},$$
$$R(\mathbf{p}, \mathbf{o}) = R(\mathbf{o}, \mathbf{p}) = \mathbf{p} \cdot \mathbf{o},$$
$$R(\mathbf{s}, \mathbf{o}) = R(\mathbf{o}, \mathbf{s}) = \mathbf{s} \cdot \mathbf{o}; \tag{4}$$

therefore

$$R_2 = R_1'. \tag{5}$$

This structure of the Jones matrix for the sandwich is quite useful in the analysis of the liquid-crystal cell optical characteristics. In Section 3 we shall make use of this matrix to derive the generalized Jones matrix of the twist cell with arbitrary director orientation and viewing angles.

3. GENERALIZED 2 × 2 JONES MATRIX OF A LIQUID-CRYSTAL CELL AT OBLIQUE ANGLE OF INCIDENCE

If we consider the liquid-crystal medium as a stack of N homogeneous uniaxial plates, the total propagation matrix can be approximated as a product of propagation matrices of the kind discussed in Section 2:

$$J = J_N J_{N-1} \cdots J_n \cdots J_3 J_2 J_1, \tag{6}$$

where

$$J_n = [R_2 G R_1]_n, \tag{7}$$

$$\begin{pmatrix} \mathbf{E}_{Np}' \\ \mathbf{E}_{Ns}' \end{pmatrix} = J \begin{pmatrix} \mathbf{E}_{1p} \\ \mathbf{E}_{1s} \end{pmatrix}. \tag{8}$$

Here J_n is the Jones matrix of the nth layer as expressed in Eq. (2), and $\mathbf{E}_{1p}$, $\mathbf{E}_{1s}$ and $\mathbf{E}_{Np}'$, $\mathbf{E}_{Ns}'$ are the electric field's **p** and **s** components at the input and the output wave, respectively.

In Eqs. (6) and (7), it is assumed that the isotropic layers do not introduce additional optical reflection, refraction, and phase retardation because of their zero thickness. Without any loss of generality, we can always choose the Cartesian coordinate system such that the incident light wave vector $\mathbf{K}_i$ lies on the x–z plane and the x–y plane is parallel to the substrate surface. Figure 1 shows the geometry of the system, and Fig. 2 shows the relationship between the various vectors on the surface plane of the liquid-crystal cell. $\mathbf{D}_1$ and $\mathbf{D}_2$ are the input and output director orientations. $\mathbf{P}_1$ and $\mathbf{P}_2$ are the polarizer and the analyzer. The direction of the $+z$ axis

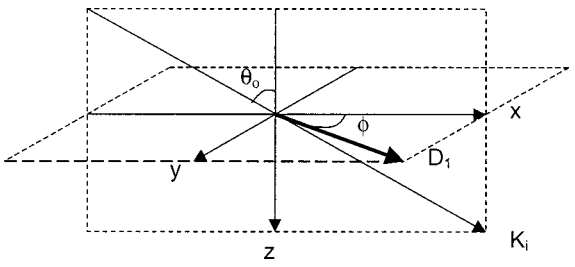

Fig. 1. Geometry of the input light.

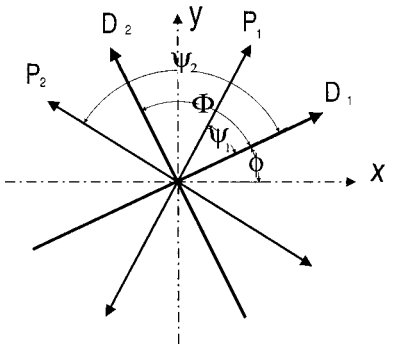

Fig. 2. Definition of various angles in the general twist cell.

points from the entrance polarizer to the exit analyzer. The input director of the liquid-crystal cell, $\mathbf{D}_1$, is at an angle of ϕ to the x axis. All the other angles are referenced to this input director. The total twist angle of the liquid-crystal cell is Φ. The polar angle of the optical axis of the first birefringent plate relative to the x axis will be $\phi_1 = \phi$, and that of the last plate will be $\phi_N = \phi + \Phi$. If no voltage is applied to the LCD, ϕ_n changes linearly so that the twist angle between adjacent birefringent plates will be $\Phi/(N-1)$. In general, ϕ_n should be obtained numerically by minimizing Frank's energy in the presence of an electric field.[14,15] Suppose that the incident light impinges on the x–z plane at an oblique angle θ_o; then $\mathbf{K}_i$ is given by

$$\mathbf{K}_i = [\sin\theta_o \quad 0 \quad \cos\theta_o]. \tag{9}$$

The **s** and **p** vectors in the fictitious isotropic medium in any layer are always constant and can be expressed as

$$\mathbf{s} = [0 \quad -1 \quad 0], \tag{10}$$

$$\mathbf{p} = \frac{\mathbf{K}_i \times \mathbf{s}}{|\mathbf{K}_i \times \mathbf{s}|} = [\cos\theta_o \quad 0 \quad -\sin\theta_o]. \tag{11}$$

The wave vectors of the **e** and **o** waves in the nth birefringent layer are given by

$$\mathbf{K}_o = [\sin\theta_o \quad 0 \quad \cos\theta_o], \tag{12}$$

$$\mathbf{K}_e = [n_o \sin\theta_o \quad 0 \quad n_e(\theta_e)\cos\theta_e] \tag{13}$$

where

$$\cos\theta_e = \sigma_{ez}/n_e(\theta_e), \tag{14}$$

θ_e is the refractive angle of the **e** wave in the uniaxial medium, and $n_e(\theta_e)$ is the refractive index of the **e** wave along the θ_e direction. We have chosen the refractive index of the fictitious isotropic medium to be n_o, so that there is no refraction for the **o** wave. Now the director orientation in the nth layer is given by

$$\mathbf{D}_n = [\cos\phi_n \cos\theta_n \quad \sin\phi_n \cos\theta_n \quad \sin\theta_n], \tag{15}$$

where ϕ_n is the polar angle and θ_n is the tilt angle of the liquid-crystal director in the nth layer. The unit **o** vector in the uniaxial medium is given by

$$\mathbf{o} = \frac{\mathbf{D}_n \times \mathbf{K}_o}{|\mathbf{D}_n \times \mathbf{K}_o|} = \left[\frac{\sin\phi_n \cos\theta_n \cos\theta_o}{A_o} \quad \frac{\sin\theta_n \sin\theta_o - \cos\phi_n \cos\theta_n \cos\theta_o}{A_o} \quad \frac{-\sin\phi_n \cos\theta_n \sin\theta_o}{A_o} \right], \tag{16}$$

and, provided that $|n_e - n_o| \ll n_o, n_e$, the refraction angles θ_o and θ_e are almost equal (i.e., $\theta_e \cong \theta_o$) and the $\mathbf{e}$ vector can be given approximately by

$$\mathbf{e} = \frac{\mathbf{K}_e \times \mathbf{o}}{|\mathbf{K}_e \times \mathbf{o}|} = \left[\frac{n_e(\theta_e)(\cos\theta_e)(\cos\phi_n \cos\theta_n \cos\theta_o - \sin\theta_n \sin\theta_o)}{A_e} \quad \frac{(\sin\phi_n \cos\theta_n)[n_o \sin^2\theta_o + n_e(\theta_e)\cos\theta_e \cos\theta_o]}{A_e} \quad \frac{-n_o(\sin\theta_o)(\cos\phi_n \cos\theta_n \cos\theta_o - \sin\theta_n \sin\theta_o)}{A_e} \right]. \tag{17}$$

In Eqs. (16) and (17) the normalization constants A_o and A_e are given by

$$A_o = [\sin^2\phi_n \cos^2\theta_n + (\cos\phi_n \cos\theta_n \cos\theta_o - \sin\theta_n \sin\theta_o)^2]^{1/2}, \tag{18}$$

$$A_e = \{[{n_o}^2 \sin^2\theta_o + {n_e}^2(\theta_e)\cos^2\theta_e]\Delta^2 + (\sin^2\phi_n \cos^2\theta_n) \times [n_o \sin^2\theta_o + n_e(\theta_e)\cos\theta_e \cos\theta_o]^2\}^{1/2}, \tag{19}$$

where

$$\Delta = \cos\phi_n \cos\theta_n \cos\theta_o - \sin\theta_n \sin\theta_o. \tag{20}$$

The two eigenvalues in the uniaxial medium are given by[8]

$$\sigma_{ez} = \frac{({n_e}^2 - {n_o}^2)\sin\theta_n \cos\theta_n \cos\phi_n \sin\theta_o}{{n_o}^2 + ({n_e}^2 - {n_o}^2)\sin^2\theta_n} + \frac{n_o n_e}{{n_o}^2 + ({n_e}^2 - {n_o}^2)\sin^2\theta_n} \times \left\{ {n_o}^2 + ({n_e}^2 - {n_o}^2)\sin^2\theta_n - \left[1 - \frac{{n_e}^2 - {n_o}^2}{{n_e}^2}\cos^2\theta_n \sin^2\phi_n \right]\sin^2\theta_o \right\}^{1/2}, \tag{21}$$

$$\sigma_{oz} = ({n_o}^2 - \sin^2\theta_o)^{1/2}. \tag{22}$$

Finally, the elements of the transformation matrix $\mathbf{R}_1$ can be obtained as

$$R(\mathbf{p}, \mathbf{e}) = \frac{[n_o \sin^2\theta_o + n_e(\theta_e)\cos\theta_e \cos\theta_o](\cos\phi_n \cos\theta_n \cos\theta_o - \sin\theta_n \sin\theta_o)}{A_e}, \tag{23}$$

$$R(\mathbf{s}, \mathbf{e}) = -\frac{(\sin\phi_n \cos\theta_n)[n_o \sin^2\theta_o + n_e(\theta_e)\cos\theta_e \cos\theta_o]}{A_e}, \tag{24}$$

$$R(\mathbf{p}, \mathbf{o}) = \frac{\sin\phi_n \cos\theta_n}{A_o}, \tag{25}$$

$$R(\mathbf{s}, \mathbf{o}) = \frac{\cos\phi_n \cos\theta_n \cos\theta_o - \sin\theta_n \sin\theta_o}{A_o}. \tag{26}$$

Thus all the parameters of the Jones matrix can be expressed in terms of the liquid-crystal cell parameters and the incidence light angles. We can now use the above equations to calculate the optical properties of any LCD at any incidence angle.

4. SOME SPECIAL CASES

There are many cases where the generalized 2 × 2 Jones matrix derived above can be reduced to the standard expressions. We first examine these special cases before performing full calculations of light transmission for general STN liquid-crystal cells.

A. Normal Incidence

In this case $\phi = 0$ and $\theta_o = 0$; thus $\theta_e = 0$. Then we have

$$R_1 = \begin{bmatrix} \cos\phi_n & -\sin\phi_n \\ \sin\phi_n & \cos\phi_n \end{bmatrix}, \tag{27}$$

which is simply the rotation Jones matrix, and

$$\sigma_{ez} = \frac{n_o n_e}{[{n_o}^2 + ({n_e}^2 - {n_o}^2)\sin^2\theta_n]^{1/2}}, \tag{28}$$

$$\sigma_{oz} = n_o \tag{29}$$

are the eigenvalues. It can be shown easily that Eq. (6) will simply lead to the ordinary Jones matrix as presented in many previous papers.[13,16] In particular, it can be shown that the representations of Eqs. (6) and (7) are equivalent to the expressions given by Lien in Ref. 11.

B. Liquid-Crystal Cell with Small Δn

In this case we assume that $n_e \approx n_o$ and $\theta_e \approx \theta_o$; thus

$$A_o = [\sin^2 \phi_n \cos^2 \theta_n + (\cos \phi_n \cos \theta_n \cos \theta_o - \sin \theta_n \sin \theta_o)^2]^{1/2}, \quad (30)$$

$$A_e = n_o A_o, \quad (31)$$

$$R_1 = \begin{bmatrix} \dfrac{\cos \phi_n \cos \theta_n \cos \theta_o - \sin \theta_n \sin \theta_o}{A_o} & -\dfrac{\sin \phi_n \cos \theta_n}{A_o} \\ \dfrac{\sin \phi_n \cos \theta_n}{A_o} & \dfrac{\cos \phi_n \cos \theta_n \cos \theta_o - \sin \theta_n \sin \theta_o}{A_o} \end{bmatrix}. \quad (32)$$

C. Liquid-Crystal Cell with No Twist and Nonuniform Tilt Angle at Normal Incidence

In this case $\phi_n = 0$ and $\theta_o = 0$, but θ_n is still allowed to vary. This will be the case, for example, in hybrid aligned nematic cells, pi-cells, etc. From Eq. (18) we have

$$A_o = \cos \theta_n. \quad (33)$$

The transformation matrix becomes the unity matrix

$$R_1 = \begin{bmatrix} 1 & 0 \\ 0 & 1 \end{bmatrix}, \quad (34)$$

and

$$\sigma_{ez} = \frac{n_o n_e}{[n_o^2 + (n_e^2 - n_o^2)\sin^2 \theta_n]^{1/2}}, \quad (35)$$

$$\sigma_{oz} = n_o. \quad (36)$$

The Jones matrix can then be written as

$$J = \begin{bmatrix} \exp\left(-ik \sum_{i=1}^{N} \sigma_{ez} h\right) & 0 \\ 0 & \exp(-ik\sigma_{oz} d) \end{bmatrix}, \quad (37)$$

where d is the thickness of the liquid-crystal cell. This is simply the Jones matrix of a retardation plate.

D. Liquid-Crystal Cell with No Twist and Uniform Tilt Angle

This is a uniform homogeneously aligned electrically controlled birefringence cell. In this case, if we vary θ_o but keep $\phi = 0$, then

$$\sigma_{ez} = \frac{(n_e^2 - n_o^2)\sin \theta_n \cos \theta_n}{n_o^2 + (n_e^2 - n_o^2)\sin^2 \theta_n} \sin \theta_o + \frac{n_o n_e}{n_o^2 + (n_e^2 - n_o^2)\sin^2 \theta_n} \times [n_o^2 + (n_e^2 - n_o^2)\sin^2 \theta_n - \sin^2 \theta_o]^{1/2}, \quad (38)$$

$$\sigma_{oz} = (n_o^2 - \sin^2 \theta_o)^{1/2}. \quad (39)$$

The Jones matrix is given by

$$J = \begin{bmatrix} \exp(-ik\sigma_{ez} d) & 0 \\ 0 & \exp(-ik\sigma_{oz} d) \end{bmatrix}, \quad (40)$$

which is again the Jones matrix of a retardation plate. It follows that when $\Psi_1 = -45°$ and $\Psi_2 = +45°$, the intensity distribution of the output light can be expressed as

$$I = \frac{1}{2} \sin^2 \left[\frac{\pi}{\lambda}(\sigma_{ez} - \sigma_{oz}) d\right]. \quad (41)$$

This result is the same as that usually used for the measurement of the pretilt angle of a parallel aligned liquid-crystal cell.[17–20]

5. AIR–POLARIZER–GLASS–LIQUID-CRYSTAL BOUNDARIES

To completely formulate the problem of calculating the transmission of the liquid-crystal cell at oblique angle of incidence, we still need to take into account the air–polarizer–glass–liquid-crystal boundaries. The transformation matrix for all the interfaces at the entrance plane is given by

$$\begin{pmatrix} \mathbf{E}_{1p} \\ \mathbf{E}_{1s} \end{pmatrix} = \begin{bmatrix} T_{pg-l} & 0 \\ 0 & T_{sg-l} \end{bmatrix} \begin{bmatrix} T_{pp-g} & 0 \\ 0 & T_{sp-g} \end{bmatrix} \times \begin{bmatrix} \cos^2(\psi_1 + \phi) & \sin(\psi_1 + \phi)\cos(\psi_1 + \phi) \\ \sin(\psi_1 + \phi)\cos(\psi_1 + \phi) & \sin^2(\psi_1 + \phi) \end{bmatrix} \begin{bmatrix} T_{pa-p} & 0 \\ 0 & T_{sa-p} \end{bmatrix} \begin{pmatrix} \mathbf{E}_{\text{air } p} \\ \mathbf{E}_{\text{air } s} \end{pmatrix}, \quad (42)$$

where

$$T_{pa-p} = \frac{[\sin(2\theta_{\text{air}})\sin(2\theta_p)]^{1/2}}{\sin(\theta_{\text{air}} + \theta_p)\cos(\theta_{\text{air}} - \theta_p)}, \quad (43)$$

$$T_{sa-p} = \frac{[\sin(2\theta_{\text{air}})\sin(2\theta_p)]^{1/2}}{\sin(\theta_{\text{air}} + \theta_p)} \quad (44)$$

are the Fresnel transmission coefficients of the **p** and **s** components at the air–polarizer interface. $\mathbf{E}_{\text{air}\,p}$ and $\mathbf{E}_{\text{air}\,s}$ are the electric field components in air. In Eq. (42) we have assumed a perfect polarizer oriented at an angle Ψ_1 to the director angle at the input plane. θ_{air} is the incidence angle of the light in air. θ_p is the refractive angle of the light in the polarizer. θ_p can be written as

$$\theta_p = \sin^{-1}[n_{\text{air}}(\sin\theta_{\text{air}})/n_p], \quad (45)$$

where n_p is the refractive index of the glass plate. The Fresnel transmission coefficients of the **p** and **s** components at the polarizer–glass interface, T_{pp-g} and T_{sp-g}, can be obtained by replacing θ_{air} with θ_p and θ_p with θ_g in Eqs. (43) and (44). Here θ_g can be derived by replacing n_p with n_g and n_{air} with n_g in Eq. (45). T_{pg-l} and T_{sg-l} can be derived in the same manner. Similarly, at the exit surface, the transformation matrix is given by

$$\begin{pmatrix} \mathbf{E}'_{\text{air}\,p} \\ \mathbf{E}'_{\text{air}\,s} \end{pmatrix} = \begin{bmatrix} T_{pp-a} & 0 \\ 0 & T_{sp-a} \end{bmatrix} \begin{bmatrix} \cos^2(\psi_2 + \phi) & \sin(\psi_2 + \phi)\cos(\psi_2 + \phi) \\ \sin(\psi_2 + \phi)\cos(\psi_2 + \phi) & \sin^2(\psi_2 + \phi) \end{bmatrix} \times \begin{bmatrix} T_{pg-p} & 0 \\ 0 & T_{sg-p} \end{bmatrix} \begin{bmatrix} T_{pl-g} & 0 \\ 0 & T_{sl-g} \end{bmatrix} \begin{pmatrix} \mathbf{E}'_p \\ \mathbf{E}'_{Ns} \end{pmatrix}, \quad (46)$$

where

$$T_{pp-a} = \frac{[\sin(2\theta_p)\sin(2\theta_{\text{air}})]^{1/2}}{\sin(\theta_p + \theta_{\text{air}})\cos(\theta_p - \theta_{\text{air}})}, \quad (47)$$

$$T_{sp-a} = \frac{[\sin(2\theta_p)\sin(2\theta_{\text{air}})]^{1/2}}{\sin(\theta_p + \theta_{\text{air}})}. \quad (48)$$

$\mathbf{E}'_{\text{air}\,p}$ and $\mathbf{E}'_{\text{air}\,s}$ are the electric field components in the air at the exit side. The final output intensity can be found to be

$$I = \frac{\mathbf{E}^{2\prime}_{\text{air}\,p} + \mathbf{E}^{2\prime}_{\text{air}\,s}}{\mathbf{E}^2_{\text{air}\,p} + \mathbf{E}^2_{\text{air}\,s}}. \quad (49)$$

Equation (49) is slightly different from the expressions given in Refs. 7 and 8. The reason is simply that the **p** and **s** components are used as the input electric field.

6. SIMULATION RESULTS AND COMPARISON WITH OTHER METHODS

Results of LCD cell simulations with use of the exact 4×4 matrix, the Lien extended Jones matrix, and the Yeh 2×2 Jones matrix as formulated in this paper are presented here for comparison. We shall consider the case of a 90° TN LCD with E-70 as a specific example, though the generalized Jones matrix method should apply to LCD's with any twist angle. The cell parameters for this particular calculation are listed in Table 1. The polarizer angles are $\Psi_1 = 0°$ and $\Psi_2 = 90°$. This corresponds to the second minimum operation. Results of calculations of the transmission as a function of incident angles are presented in Figs. 3–8. Figures 9 and 10 present results for transmission as a function of voltage. In all the figures, the label 4 by 4 refers to the exact 4×4 matrix, 2 by 2 refers to the older version of the Lien extended Jones matrix,[11] m 2×2 refers to the new Lien extended Jones matrix, and New 2 by 2 refers to the Yeh Jones matrix as formulated in this paper.

Figure 3 shows the results of cell transmission as a function of viewing angle. No voltage is applied to the cell in these calculations. The polar angle ϕ is fixed at 0°. The results therefore show the dependence of the transmission on the azimuthal angle θ. Figure 4 shows the errors of the extended 2×2 methods as compared with that of the 4×4 method. It can be seen that in all cases the errors are less than 0.4%. The differences between the various extended Jones matrices are not great. The maximum transmission of 45.3% at normal incidence for this display is predicted by all three calculations and is due to Fresnel reflection loss from the interfaces.

Figure 5 presents similar results for the case of $\phi = -45°$. Figure 6 shows the errors of the extended 2×2 Jones matrix methods as compared with that of the exact 4×4 matrix. In all cases it can be seen that the errors are less than 0.5% for incidence angles smaller than 40°. However, the old Lien extended Jones matrix shows large errors of over 2%–3% at angles larger than

Table 1. Parameters Used in the Calculations

Parameter	Value
K_{11}	12.6×10^{-12} N
K_{22}	6.1×10^{-12} N
K_{33}	18.65×10^{-12} N
$\epsilon_{\parallel}$	108.26×10^{-12} F/m
$\epsilon_{\perp}$	42.05×10^{-12} F/m
n_o	1.5269
n_e	1.7142
Twist angle ϕ	90°
Cell gap d	5.3 μm
Chiral pitch P	20 μm
Pretilt angle θ_s	2°
Wavelength λ	0.555 μm
Polarizer refractive n_o	$1.5 + 2.2 \times 10^{-5}i$
Polarizer refractive n_e	$1.5 + 1.5 \times 10^{-5}i$
Polarizer thickness d_p	190 μm
Glass refractive index n_g	1.5
Glass thickness d_g	1 mm

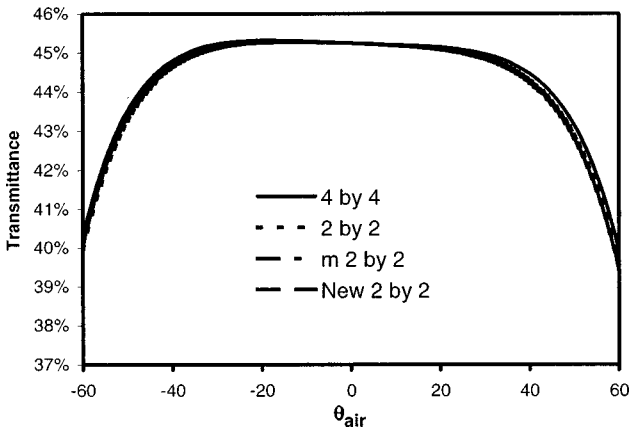

Fig. 3. Comparison of optical transmission as a function of incidence angle θ_{air} calculated by three methods for a 90° TN cell filled with E-70. The incident light polar angle is $\phi = 0°$. In this and the following figures, 2 by 2 refers to the 2×2 Jones matrix in Ref. 11, m 2 by 2 refers to the 2×2 Jones matrix in Ref. 12, New 2 by 2 refers to the Jones matrix derived in this paper, and 4 by 4 refers to the full 4×4 Berreman matrix.

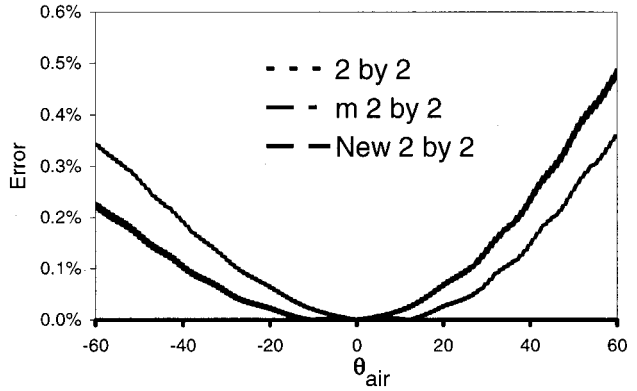

Fig. 4. Absolute errors of the 2×2 methods as compared with that of the 4×4 method for the case of Fig. 3.

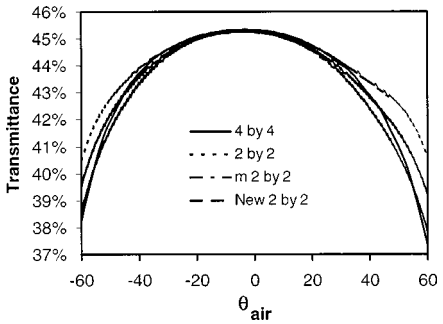

Fig. 5. Comparison of optical transmission as a function of incidence angle θ_{air} calculated by three methods for a 90° TN cell filled with E-70. The incident light polar angle is $\phi = -45°$.

60°. The results of the new Yeh Jones matrix show a maximum of 0.6% error in the same range, while the new Lien Jones matrix shows large errors at angles larger than 45°. It should be noted that the older version of the Lien extended Jones matrix has been applied to commercial numerical simulation packages. Obviously, some corrections are needed for calculations using those packages.

Figure 7 shows the simulation results for a polar angle ϕ of +45°. The azimuthal angle θ is varied as in the previous cases. Figure 8 shows the errors of the 2×2 methods as compared with that of the 4×4 method. It can be seen that in all cases the errors are less than 0.8% in the range of angles studied. In some cases the Lien extended Jones matrix is better, while in other cases the Yeh extended Jones matrix is better.

Figures 3–8 were generated for $V = 0$. For the sake of completeness, dynamic simulation with an applied voltage was also performed. The director deformation is first calculated by using the hydrodynamic equations. The Euler–Lagrange equations for the director deformation were solved to give the director angles $\phi(z)$ and $\theta(z)$ for

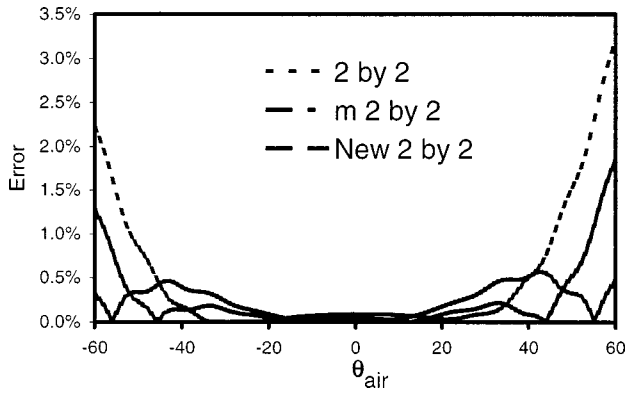

Fig. 6. Absolute errors of the 2×2 methods as compared with that of the 4×4 method for the case of Fig. 5.

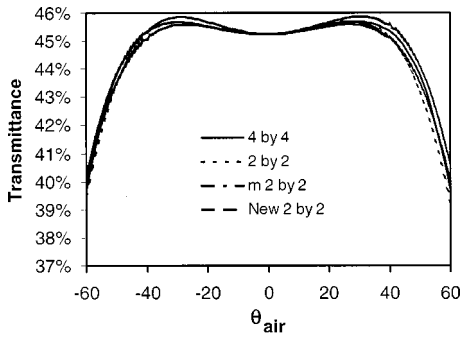

Fig. 7. Comparison of optical transmission as a function of incidence angle θ_{air} calculated by three methods for a 90° TN cell filled with E-70. The incident light polar angle is $\phi = 45°$.

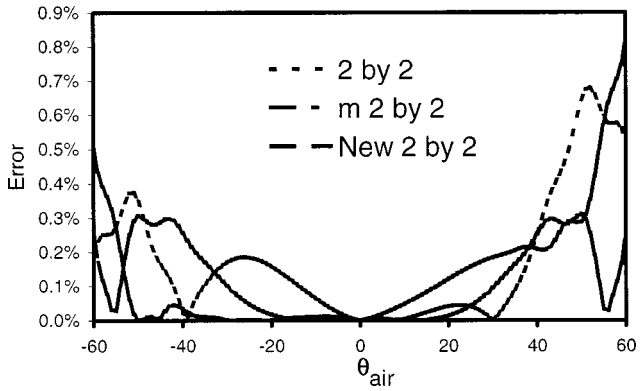

Fig. 8. Absolute errors of the 2×2 methods as compared with that of the 4×4 method for the case of Fig. 7.

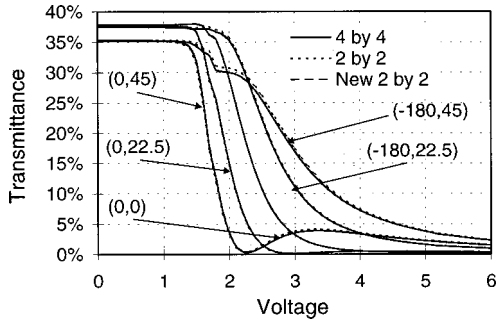

Fig. 9. Three sets of curves comparing optical transmission as a function of applied voltage calculated by three methods for viewing angles of $(\phi, \theta_i) = (0°, 0°)$, $(0°, 22.5°)$, $(0°, 45°)$, $(-180°, 22.5°)$, and $(-180°, 45°)$.

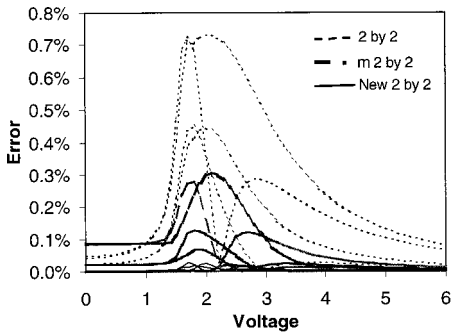

Fig. 10. Comparison of absolute errors for the various cases depicted in Fig. 9.

all values of z inside the liquid-crystal cell for any value of applied voltage.[21] The transmission is then calculated by dividing the LCD cell into sections as in the case of zero applied voltage. In this calculation the viewing angles are fixed, and the applied voltage is varied to obtain the complete transmission–voltage characteristics.

The transmission as a function of the applied voltage for the viewing angles of $(\phi, \theta_i) = (0°, 0°)$, $(0°, 22.5°)$, $(0°, 45°)$, $(-180°, 22.5°)$, and $(-180°, 45°)$ of a 90° TN cell were calculated and are shown in Fig. 9. Comparing the three sets of curves in Fig. 9, one can see that the results obtained from all three methods are very close to each other. Figure 10 shows the absolute errors of the extended Jones matrices relative to that of the 4×4 matrix method as calculated in Fig. 9. It can be seen that the Yeh extended Jones matrix is dramatically more accurate than the extended Jones matrix in approximating the exact 4×4 matrix method.

In all cases the maximum error occurs near the Frederick transition voltage, which is near 2 V in the present situation. In Fig. 10 the dashed curves represent the old Lien extended Jones matrix. It is seen that the absolute error can be as high as 0.7%. The dotted–dashed gray curves are results for the new Lien Jones matrix. The maximum error has reduced to 0.3%. For the Yeh Jones matrix as formulated here, the maximum error is less than 0.05%, which is remarkable. For all intents and purposes, the Yeh extended Jones matrix is identical to the 4×4 Berreman matrix in modeling the LCD. In this dynamic calculation, a 2×2 approximation to the 4×4 matrix is necessary because of the vast amount of calculations involved. Even with a fast computer, Fig. 9 took a long time to generate, especially for the 4×4 case. Thus the power of the extended Jones matrix is clearly demonstrated.

7. CONCLUSIONS

In this paper we have presented a detailed formulation of the Yeh extended 2×2 Jones matrix representation for TN LCD's at oblique angles of incidence. The boundary-matching conditions are taken care of by optical reflection and refraction from fictitious isotropic layers between the birefringent plates. This method is rather intuitive and can be used to calculate the viewing angles of LCD cells. An extension of this method to some special cases was also given.

We have also performed numerical comparisons of this Yeh extended Jones matrix and the Lien extended Jones matrix in both its earlier and its more recent renditions. It is shown that numerical results of these 2×2 extended Jones matrices, as compared with those of the exact 4×4 matrix, are quite favorable. In most cases the errors are generally quite small. From the numerical results, it was also seen that the Yeh formulation is generally better in accuracy than the Lien formulation.

The Yeh extended Jones matrix can yield numerical results that are very close to the exact 4×4 values. This method is fast, direct, and simple. It is also physically more intuitive, with all the electric field and magnetic field boundary conditions taken into account implicitly. The employment of fictitious zero-thickness layers indeed simplifies the physical picture considerably. When combined with the parameter space representation method,[22] this extended Jones matrix method can be used to design and optimize TN and STN LCD's. In particular, both transmittive and reflective LCD's[23–25] can be modeled accurately.

Finally, it should be noted that the extended Jones matrices of Yeh and Lien are approximations of the exact 4×4 Berreman matrix. There are also other formulations of the 4×4 matrix that may be amenable to approximations.[26] The relationship between the extended Jones matrices and these other 4×4 formulations may be of further investigative worth as well.

ACKNOWLEDGMENT

This research was supported by the Hong Kong Industry Department.

Address all correspondence to H. S. Kwok at the location on the title page or by e-mail, eekwok@ust.hk.

*Permanent address, Center for Optical and Electromagnetic Research, State Key Laboratory of Modern Optical Instrumentation, Department of Optical Engineering, Zhejiang University, Hangzhou, 310027, China.

REFERENCES

1. H. Wohler, "Numerical methods for parameter optimization of liquid crystal display," in *Proceedings of the Society for Information Display International Symposium, Santa Ana,*

California (Society for Information Display, San Jose, Calif., 1991), pp. 582–585.
2. M. Schadt and W. Helfrich, "Voltage-dependent optical activity of twisted nematic liquid crystal," Appl. Phys. Lett. **18**, 127–128 (1971).
3. T. J. Scheffer and J. Nehring, "A new highly multiplexable liquid crystal display," Appl. Phys. Lett. **45**, 1021–1023 (1984).
4. G. H. Gooch and H. A. Tarry, "The optical properties of twisted nematic liquid crystal structures with twist angles $<90°$," J. Phys. D **8**, 1575–1584 (1975).
5. D. W. Berreman, "Optics in stratified and anisotropic media: 4×4 matrix formulation," J. Opt. Soc. Am. **62**, 502–510 (1972); "Optics in smoothly varying anisotropic planar structure: application to liquid crystal twist cells," J. Opt. Soc. Am. **63**, 1374–1380 (1973).
6. H. Wöhler, G. Hass, M. Fritsch, and D. A. Mlynski, "Faster 4×4 matrix method for inhomogeneous uniaxial media," J. Opt. Soc. Am. A **5**, 1554–1557 (1988).
7. K. H. Yang, "Elimination of the Fabry–Perot effect in the 4×4 matrix method for inhomogeneous uniaxial media," J. Appl. Phys. **66**, 1550–1554 (1990).
8. P. Yeh, "Extended Jones matrix method," J. Opt. Soc. Am. **72**, 507–513 (1982).
9. P. Yeh, *Optical Waves in Layered Media* (Wiley, New York, 1988), pp. 201–253.
10. C. Gu and P. Yeh, "Extended Jones matrix method. II," J. Opt. Soc. Am. A **10**, 966–973 (1993).
11. A. Lien, "Extended Jones matrix representation for the twisted nematic liquid-crystal display at oblique incidence," Appl. Phys. Lett. **57**, 2767–2769 (1990).
12. A. Lien and C. J. Chen, "A new 2×2 matrix representation for twisted nematic liquid crystal displays at oblique incidence," Jpn. J. Appl. Phys. **35**, L1200–L1203 (1996).
13. Kanghua Lu and B. E. A. Saleh, "Reducing Berreman's 4×4 formulation of liquid crystal display optics to 2×2 Jones vector equations." Opt. Lett. **17**, 1557–1559 (1993).
14. C. J. Chen, A. Lien, and M. I. Nathan, "A general method to solve the deformation profile of chiral nematic LCDs with asymmetric pretilt," in *Society for Information Display International Symposium, Orlando, Florida* (Society for Information Display, San Jose, Calif., 1995), pp. 548–551.
15. H. J. Deuling, "Deformation pattern of twisted nematic liquid crystal layers in an electric field," Mol. Cryst. Liq. Cryst. **27**, 123–131 (1974).
16. B. E. A. Saleh and M. C. Teich, *Fundamentals of Photonics* (Wiley, New York, 1991), pp. 193–237.
17. T. J. Scheffer and J. Nehring, "Accurate determination of liquid crystal tilt bias angles," J. Appl. Phys. **48**, 1783–1792 (1977).
18. K. Y. Han, T. Miyashita, and T. Uchida, "Accurate determination and measurement error of the pretilt angle in the liquid crystal cell," Jpn. J. Appl. Phys. Part 2 **32**, L277–L279 (1993).
19. K. Y. Han, T. Miyashita, and T. Uchida, "Accurate measurement of pretilt angle in the liquid crystal cell by an improved crystal rotation method," Mol. Cryst. Liq. Cryst. **241**, 147–157 (1994).
20. K. Shrota, M. Yaginuma, K. Ishikawa, H. Takezoe, and A. Fukuda, "Modified crystal rotation method for measuring high pretilt angle in the liquid crystal cells," Jpn. J. Appl. Phys. Part 1 **34**, 4905–4906 (1995).
21. L. M. Blinov and V. G. Chigrinov, *Electrooptic Effects in Liquid Crystal Materials* (Springer-Verlag, New York, 1994).
22. H. S. Kwok, "Parameter space representation of liquid crystal display operating mode," J. Appl. Phys. **80**, 3687–3693 (1996).
23. S. T. Tang, F. H. Yu, J. Chen, M. Wong, H. C. Huang, and H. S. Kwok, "Reflective nematic liquid crystal displays. I. Retardation compensation," J. Appl. Phys. **81**, 5924–5929 (1997).
24. F. H. Yu, J. Chen, S. T. Tang, and H. S. Kwok, "Reflective nematic liquid crystal displays. II. Elimination of retardation film and rear polarizer," J. Appl. Phys. **82**, 5287–5295 (1997).
25. J. Chen, F. H. Yu, H. C. Huang, and H. S. Kwok, "Reflective supertwisted liquid crystal displays," Jpn. J. Appl. Phys., Part 1 **37**, 217–223 (1998).
26. J. Lekner, "Optical properties of a uniaxial layer," Pure Appl. Opt. **3**, 821–837 (1994).